# **Chebyshev Collocation Method for Fractional Temporary Heat Transfer Model in Composite Cylinders with Hollow Interiors**

Sh. Mohamed<sup>1,2</sup>, M. S. El-Azab<sup>1</sup>, M. Sameeh<sup>1</sup>

Corresponding author: Mona Sameeh (e-mail: eng\_mona\_2007@mans.edu.eg).

**ABSTRACT** In this paper, we propose a new spectral collocation method for the time-fractional heat equation in hollow composite cylinders. The model is based on a finite difference approximation for the time-fractional derivative, known for its computational efficiency, and a Chebyshev polynomial basis in space, which provides spectral accuracy. Its main originality consists of the rigorous a priori error estimates that demonstrate the theoretical convergence and stability of the method. The numerical simulations indicate that the scheme is an accurate and effective method for describing such complex composite systems. The results show that the present method is robust and widely applicable to advanced thermal analysis.

**INDEX TERMS** Chebyshev polynomials, Heat transfer, Collocation method, Composite cylinders, Fractional partial differential equations.

#### I. INTRODUCTION

Composite geometries are crucial in many engineering applications, as they involve more than one material within a single structure, particularly for heat conduction problems. Such composites have extensive applications in different fields, including nuclear applications [1], heat exchangers [2], ground exchanger linings [3], antenna construction [4], and for improving magnetic materials [5]. Each of these applications requires an understanding of how different materials thermally interact, especially in a complex configuration such as the hollow composite cylinders shown in Figure 1.

Conventional heat conduction models of these cylinders are typically based on integer-order differential equations, according to Fourier's law, which assumes instantaneous and direct proportionality between heat transfer and the temperature gradient. While these models effectively present hollow composite cylinders as separate layers of material, they have difficulty in accurately predicting complex thermal phenomena at the interfaces. This restriction implies strong discontinuities in temperature and heat flux, contradicting the physical coherence of the model. The increasing use of advanced composites in advanced engineering systems requires a paradigm shift in these types of advanced simulation tools.

To solve these traditional models, various methods are employed, such as the line heat-source approach [6-7], the Laplace transform method [8-9], orthogonal and quasi-orthogonal expansion techniques [10–12], the method of variable separation [13], finite integral transform approach [14], Green's function method [15-16] and meshless method [17].

However, applying fractional mathematical models to describe heat transfer has received increasing attention in recent publications, as in works [18-32]. These papers are all part of an extensive research on heat transfer in various geometries. In the references [18-22], the fractional heat transfer in slabs and plates is considered, while [23-27] focus on the fractional heat transfer in layered spheres. The problems of fractional heat transfer in cavities are discussed in [28-32]. A set of accurate and approximate methods were applied to solve fractional heat diffusion equations such as the Fourier transform [18,21], integral transform [19,21,28,30], Green's function approach[20], superposition method[22], variable separation [23,26], Laplace transform [25,29], implicit finite difference method [27], Fourier series [31, 32].

The Caputo derivative is shown to be a promising option for simulating the fractional-heat conduction in such cylinders. It provides an insight into heat spreading and thermal coupling within layers, and it accounts for the

Department of Mathematics and Engineering Physics, Faculty of Engineering, Mansoura University, 35516, Mansoura, Egypt.

<sup>&</sup>lt;sup>2</sup> Department of Basic Science, Delta Higher Institute for Engineering and Technology, Mansoura 35681, Egypt.



memory dependence. Such an approach eliminates the drawbacks of classical models. It provides valuable information about time-dependent thermal behavior, allowing for consideration of initial and boundary conditions of composite materials over an extensive range. Accordingly, with respect to energy system design, the Caputo formulation is a promising candidate for optimizing designs in, for example, insulation and energy storage systems, as well as the development of advanced heat exchangers, where a thorough understanding of the complex thermal behavior of layered materials is required.

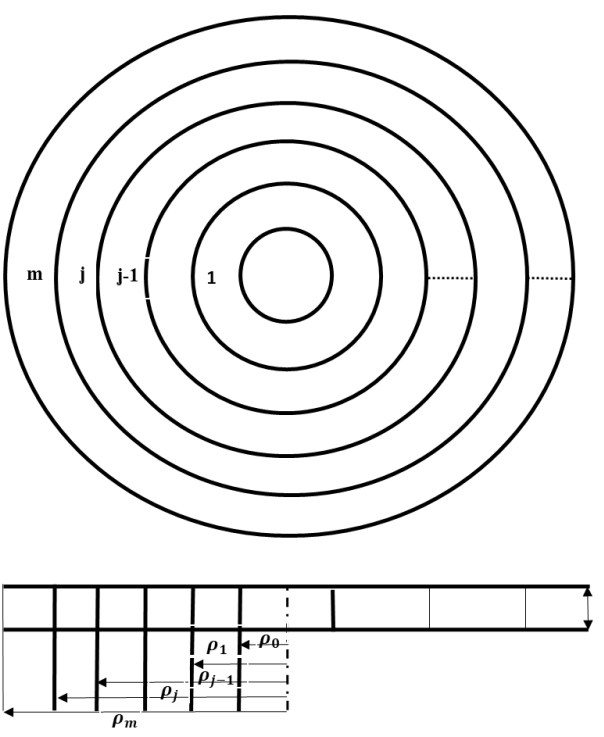


Figure 1. A hollow cylinder with an m-layer composite.

In the present paper, we consider a composite medium consisting of an m-layer cylinder with a hollow depicted in Fig. 1. Let the radius range be  $\rho_0 \le \rho \le \rho_m$ , the interior and exterior faces of the cylinder are denoted by  $\rho_0$  and  $\rho_m$ , whereas both the inside and outside radii of the  $j^{th}$  layer are marked by  $\rho_{j-1}$  and  $\rho_j$ . The following equation governs the heat conduction within the  $j^{th}$  layer:

$$\frac{1}{\mu_{j}} \frac{\partial^{\lambda} H_{j}(\rho, t)}{\partial t^{\lambda}} = \frac{\partial^{2} H_{j}(p, t)}{\partial \rho^{2}} + \frac{1}{\rho} \frac{\partial H_{j}(\rho, t)}{\partial \rho} + \frac{\omega_{j}(\rho, t)}{\sigma_{j}},$$

$$\rho_{j-1} \leq \rho \leq \rho_{j}, 1 \leq j \leq m, 0 < \lambda \leq 1$$
(1.1)

where  $H_j(\rho, t)$ ,  $\sigma_j$ ,  $\mu_j$  represent the layer's temperature, thermal conductivity, and thermal diffusivity, respectively, and  $\omega_j(\rho, t)$  Symbolizes the creation of heat inside the layer. The general form describes the boundary conditions for the cylinder's interior and exterior surfaces as follows:

$$a_{in} \frac{\partial H_1(\rho_0, t)}{\partial \rho} + b_{in} H_1(\rho_0, t) = O_{in}$$
, Page 10 (1.2)

$$a_{out} \frac{\partial H_n(\rho_n, t)}{\partial \rho} + b_{out} H_n(\rho_n, t) = O_{out}$$
 (1.3)

where  $a_{in}$ ,  $b_{in}$ ,  $a_{out}$ ,  $b_{out}$  are constants chosen carefully to satisfy possible boundary conditions, and  $O_{in}$ ,  $O_{out}$  denote the outside influences (specified temperature or thermal flux) imposed on the interior and exterior faces of the cylinder, respectively. The following conditions, guaranteeing the continuity of thermal flux and temperature at the interfaces between layers, are matched:

$$H_i(\rho_i, t) = H_{i+1}(\rho_i, t), \tag{1.4}$$

$$\sigma_{j} \frac{\partial H_{j}(\rho_{j}, t)}{\partial \rho} = \sigma_{j+1} \frac{\partial H_{j+1}(\rho_{j}, t)}{\partial \rho}, \qquad (1.5)$$

also, the initial conditions as follows

$$H_i(\rho, t = 0) = \varphi_i(\rho). \tag{1.6}$$

The temporal fractional derivative  $\frac{\partial^{\lambda} H_{j}(\rho,t)}{\partial t^{\lambda}}$ , is computed using the Caputo fractional derivative with order  $(0 < \lambda \leq 1)$  described as follows in [33]:

$$\frac{\partial^{\lambda} H(\rho,t)}{\partial t^{\lambda}} = \frac{1}{\Gamma(1-\lambda)} \int_{0}^{t} (t-s)^{-\lambda} \frac{\partial H(\rho,s)}{\partial s} ds.$$

In this study, the temperature field is expanded in terms of Chebyshev polynomials, and by enforcing the governing heat equation at collocation points, the method achieves exponential convergence rates for smooth solutions, which is well beyond what traditional finite difference or finite element approaches can achieve [34]. This high accuracy is particularly beneficial in cylindrical coordinates, where a thin layer containing the radial temperature variation maps to the standard Chebyshev interval [-1, 1] for each layer, allowing for the computation of heat flux with great precision, even for wide samples, at a minimal grid resolution. In addition, the non-uniform organization of mesh points close to the domain definition and interfaces allows this method to automatically capture high variation near the inner and outer edges of a hollow cylinder (stemming from heat conduction), thereby alleviating computational costs while guaranteeing a reliable solution for both steady-state and transient conditions throughout.

The Chebyshev collocation method can easily handle the complex situation of unfavorable layered structures with multiple layers in a single simulation, and provides a framework based on modular and scalable basis functions that can be employed to treat non-homogeneous materials with different thermal properties. We provide a domain decomposition for each layer, and only need simple algebraic constraints on the continuity of temperature and heat flux to ensure independent solutions match across layers without having the complex interface meshing required by mesh-based methods. This flexibility enables us



to handle arbitrary layer counts with only modest increases in computational complexity, as the global system remains sparse and well-conditioned due to the orthogonality of Chebyshev bases. Moreover, the proposed method has been shown to significantly simplify parametric studies, where varying layer thicknesses or conductivities can be evaluated with minimal reformulation for use in engineering applications, such as thermal insulation design or composite material optimization, where quick, high-fidelity approximations are needed.

The Chebyshev Collocation Method has been used before to solve diffusion equations in composite regions by using normal integer-order derivatives and in a single region with fractional-order derivatives. Nevertheless, the originality of the current approach lies in merging their treatment and applying the Chebyshev Collocation Method to solve the fractional transient heat conduction equations in composite cylinders with hollow cores. The resulting composite method makes it possible to effectively treat complicated geometries as well as nonlocal fractional dynamics, with high accuracy and computational efficiency. The importance of this application can be appreciated in scientific fields such as engineering science, where studies on the design of thermal insulation and optimization of composite materials require rapid, high-accuracy parametric studies to find new solutions.

The Chebyshev collocation approach is highly beneficial for a wide range of equations, including both linear and non-linear ordinary differential equations [35-37]. Partial differential equations [38-40], Troesch's problem [41], partial integro-differential equations [42], integro-differential equations [43-45], and eigenvalue problems [46]. This paper is structured in six parts, each of which is directed to a particular objective. The first section is a comprehensive summary of the study. Section 2 is devoted to introducing definitions and notation of Chebyshev polynomials. In Section 3, we propose a new approach to address the fractional transient heat transfer model in composite cylinders with hollow interiors (1.1)— (1.6). An a priori error estimation of the solution is derived in Section 4. Section 5 presents an application of the method, accompanied by specific examples. Finally, the study's main findings are summarized in Section 6.

## **II. Fundamental Relations**

Once shifted, the Chebyshev Polynomials of  $n^{th}$  degree can be correlated with  $\rho$  within the  $[\rho_{j-1}, \rho_j]$  range as stated below:

$$\psi_n^*(\rho) = \cos\left(n \arccos\left(\frac{2\rho - (\rho_j + \rho_{j-1})}{\rho_j - \rho_{j-1}}\right)\right). \tag{2.7}$$

Throughout the range  $[\rho_{j-1}, \rho_j]$ , the polynomial  $\psi_n^*(\rho)$  hits its maximum value (n+1) times, reversing its sign at each peak

$$|\psi_n|_{\infty} = 1, \qquad \psi_n(\rho_i) = (-1)^i,$$

where the norm  $\|\psi_n\|_{\infty}$  is defined as the maximum norm, as it represents the maximum value of  $|\psi_n(\rho)|$ . The Chebyshev collocation points, labeled  $\rho_i$ , are established by:

$$\rho_{i} = \frac{\rho_{j} - \rho_{j-1}}{2} \left[ \left( \frac{\rho_{j} + \rho_{j-1}}{\rho_{j} - \rho_{j-1}} \right) + \cos\left(\frac{i\pi}{n}\right) \right],$$

$$i = 0, 1, 2, \dots, n. \tag{2.8}$$

By employing the shifted first-type Chebyshev function  $\psi_n^*(\rho)$  within the interval  $[\rho_{j-1}, \rho_j]$ , the estimation of  $H(\rho)$  is achieved using a truncated shifted Chebyshev sequence, outlined as:

$$H(\rho) = \sum_{s=0}^{N} q_s^* \psi_s^*(\rho), \, \rho_{j-1} \le \rho \le \rho_j.$$
 (2.9)

The integer order derivatives are formulated similarly as follows:

$$H^{(r)}(\rho) = \sum_{s=0}^{N} q_s^{*(r)} \psi^*(\rho), \ \rho_{j-1} \le \rho \le \rho_j.$$
 (2.10)

The function  $H(\rho)$  and its derivatives are represented in a matrix form as follows:

$$H(\rho) = \psi^*(\rho) \ Q^*$$
, (2.11)

$$H^{(r)}(\rho) = \psi^*(\rho) Q^{*(r)},$$
 (2.12)

where

$$\psi^*(\rho) = [\psi_0^*(\rho) \quad \psi_1^*(\rho) \quad \psi_2^*(\rho) \cdots \ \psi_n^*(\rho)],$$
 
$$Q^* = [\frac{1}{5} q_0^* \ q_1^* \ \cdots \ q_n^*]^{\mathsf{T}}.$$

**Lemma 2.1.** [37] The derivation of the vector  $Q^{*(r)}$  from vector  $Q^*$  is accomplished through the formula:

$$Q^{*(r)} = \left(\frac{4}{\rho_i - \rho_{i-1}}\right)^{\lambda} D^r Q^*, \tag{2.13}$$

where

$$D = \begin{bmatrix} 0 & \frac{1}{2} & 0 & \frac{3}{2} & 0 & \frac{5}{2} & \dots & d_1 \\ 0 & 0 & 2 & 0 & 4 & 0 & \dots & d_2 \\ 0 & 0 & 0 & 3 & 0 & 5 & \dots & d_3 \\ \vdots & \vdots & \vdots & \vdots & \vdots & \vdots & \ddots & \vdots \\ 0 & 0 & 0 & 0 & 0 & 0 & \dots & n \\ 0 & 0 & 0 & 0 & 0 & 0 & \dots & 0 \end{bmatrix}$$

$$d_1 = \frac{n}{2}$$
,  $d_2 = 0$ ,  $d_3 = n$ , for odd  $n$ ,

where



$$d_1 = 0$$
,  $d_2 = n$ ,  $d_3 = 0$ , for even  $n$ .

This leads to the explanation of  $H^{(r)}(\rho)$  as follows:

$$H^{(r)}(\rho) = \left(\frac{4}{\rho_j - \rho_{j-1}}\right)^r \psi^*(\rho) D^r Q^* \qquad (2.14)$$

## III. Methodology explanation

For the inner  $j^{th}$  layer of m layer hollow composite cylinder, the Chebyshev collocation approach is systematically introduced with discretized governing equations at Chebyshev collocation points within the  $[\rho_{i-1}, \rho_i]$  to establish an associated discrete Chebyshev system. The related methodology is also elaborated with the other layers of the composite cylinder, with equations and boundary conditions considering their material properties and geometrical layouts. The discrete Chebyshev systems for each layer are then assembled into a global system while maintaining continuity across the layer interfaces. Such integration is essential, as these dependencies in the thermal behavior among all layers establish a complete knowledge of the composite structure for modeling purposes. Finally, this complete system is solved to obtain the overall thermal response of the composite cylinder and understand its transient heat transfer behavior.

We commence by segmenting time into a lattice with  $t_{\kappa} = \kappa \, \delta t$ , where  $\delta t$  is the prescribed time step. The Caputo fractional derivative of  $H_j(\rho, t)$  at the coordinates  $(\rho, t_{\kappa})$  is formulated as:

$$\frac{\partial^{\lambda} H_{j}(\rho, t_{\kappa})}{\partial t^{\lambda}} = \frac{1}{\Gamma(1-\lambda)} \sum_{L=0}^{\kappa-1} \int_{t_{L}}^{t_{L+1}} (t-u)^{-\lambda} \frac{\partial H_{j}(\rho, u)}{\partial u} dt. \quad (3.15)$$

Using the Traditional first-order finite difference method results in the following formulation :

$$\frac{\partial^{\lambda} H_{j}}{\partial t^{\lambda}}(\rho, t_{\kappa}) \approx D_{\kappa}^{\lambda} H_{j}(\rho, t_{\kappa})$$

$$= \frac{1}{\Gamma(1-\lambda)} \sum_{L=0}^{\kappa-1} \frac{H_{j}^{L+1} - H_{j}^{L}}{\delta t} \int_{t_{L}}^{t_{L+1}} (t - u)^{-\lambda} du = \frac{1}{\delta t^{\lambda} \Gamma(2-\lambda)} \sum_{L=0}^{\kappa-1} \alpha_{\kappa-L} (H_{j}^{L+1} - H_{j}^{L}), \quad (3.16)$$

here  $H_j^L$  stands for  $H_j(\rho, t_L)$ , and  $\alpha_L = L^{1-\lambda} - (L-1)^{1-\lambda}$ . We obtain an alternate formulation by adjusting equation (3.16):

$$\frac{\partial^{\lambda} H_{j}}{\partial t^{\lambda}}(\rho, t_{\kappa}) = \frac{1}{\delta t^{\lambda} \Gamma(2-\lambda)} \sum_{L=0}^{\kappa-1} \beta_{L} (H_{j}^{\kappa-L} - H_{j}^{\kappa-L-1}), \quad (3.17)$$
here
$$\beta_{L} = (L+1)^{1-\lambda} - L^{1-\lambda}.$$

Equation (1.1) in its discretized form is written as: Page 12

$$\frac{1}{\delta t^{\lambda} \mu_{j} \Gamma(2-\lambda)} \sum_{L=0}^{\kappa-1} \beta_{L} (H_{j}^{\kappa-L} - H_{j}^{\kappa-L-1})$$

$$= (H_{j}'')^{\kappa} + \frac{1}{\rho} (H_{j}')^{\kappa} + \frac{\omega_{j}(\rho, t_{\kappa})}{\sigma_{j}},$$
(3.18)

This might be reduced to

$$\delta t^{\lambda} \mu_{j} \Gamma(2-\lambda) \left(H_{j}^{"}\right)^{\kappa} + \frac{1}{\rho} \delta t^{\lambda} \mu_{j} \Gamma(2-\lambda) \left(H_{j}^{'}\right)^{\kappa} - H_{j}^{\kappa}$$

$$= F_{j}^{\kappa}(\rho)$$
(3.19)

where

$$F_{j}^{\kappa}(\rho) = \sum_{L=0}^{\kappa-1} \beta_{L} \left( H_{j}^{\kappa-L} - H_{j}^{\kappa-L-1} \right) - H_{j}^{\kappa-1} - \delta t^{\lambda} \mu_{j} \Gamma(2-\lambda) \frac{\omega_{j}(\rho, t_{\kappa})}{\sigma_{j}}.$$

$$(3.20)$$

**Theorem 3.1**: Implementing the proposed Chebyshev approximation (2.9) in solving equation (3.19) produces the following discrete Chebyshev system.

$$\delta t^{\lambda} \mu_{j} \Gamma(2-\lambda) \left(\frac{4}{\rho_{j} - \rho_{j-1}}\right)^{2} \psi_{j}^{*}(\rho_{i}) D^{2} \left(Q_{j}^{*}\right)^{\kappa} + \frac{1}{\rho_{i}} \delta t^{\lambda} \mu_{j} \Gamma(2-\lambda) \left(\frac{4}{\rho_{j} - \rho_{j-1}}\right) \psi_{j}^{*}(\rho_{i}) D\left(Q_{j}^{*}\right)^{\kappa} - \psi_{j}^{*}(\rho_{i}) \left(Q_{j}^{*}\right)^{\kappa} = F_{j}^{\kappa}(\rho_{i})$$
(3.21)

The discrete Chebyshev system, based on Chebyshev collocation nodes  $\rho_i$ , is formulated in the following matrix representation:

$$W_j^{\kappa} \left( Q_i^* \right)^{\kappa} = F_j^{\kappa} \,, \tag{3.22}$$

where

$$W_{j}^{\kappa} = \delta t^{\lambda} \, \mu_{j} \, \Gamma(2 - \lambda) \left(\frac{4}{\rho_{j} - \rho_{j-1}}\right)^{2} \psi_{j}^{*} D^{2} + V \, \delta t^{\lambda} \, \mu_{j} \, \Gamma(2 - \lambda) \left(\frac{4}{\rho_{j} - \rho_{j-1}}\right) \psi_{j}^{*} \, D - \psi_{j}^{*} \, ,$$
(3.23)

and

$$\psi_{j}^{*} = \begin{bmatrix} (\psi_{0}^{*})_{j} (\rho_{0}) & (\psi_{1}^{*})_{j} (\rho_{0}) & \cdots & (\psi_{N}^{*})_{j} (\rho_{0}) \\ (\psi_{0}^{*})_{j} (\rho_{1}) & (\psi_{1}^{*})_{j} (\rho_{1}) & \cdots & (\psi_{N}^{*})_{j} (\rho_{1}) \\ \vdots & \vdots & \ddots & \vdots \\ (\psi_{0}^{*})_{j} (\rho_{N}) & (\psi_{1}^{*})_{j} (\rho_{N}) & \cdots & (\psi_{N}^{*})_{j} (\rho_{N}) \end{bmatrix},$$



$$F_{j}^{\kappa} = \begin{bmatrix} F_{j}^{\kappa} (x_{0}) \\ F_{j}^{\kappa} (x_{1}) \\ \vdots \\ F_{j}^{\kappa} (x_{N}) \end{bmatrix}, \qquad V = \begin{bmatrix} \frac{1}{\rho_{0}} & 0 & 0 & \cdots & 0 \\ 0 & \frac{1}{\rho_{1}} & 0 & \cdots & 0 \\ 0 & 0 & \frac{1}{\rho_{3}} & \cdots & 0 \\ \vdots & \vdots & \vdots & \ddots & \vdots \\ 0 & 0 & 0 & \cdots & \frac{1}{\rho_{N}} \end{bmatrix}$$

Each layer's discrete Chebyshev systems are subsequently combined to form a global system as follows:

$$W^{\kappa} (Q^*)^{\kappa} = F^{\kappa}, \qquad (3.24)$$

where

$$W^{\kappa} = \begin{bmatrix} W_1^{\kappa} & 0 & 0 & \cdots & 0 & 0 \\ 0 & W_2^{\kappa} & 0 & \cdots & 0 & 0 \\ 0 & 0 & W_3^{\kappa} & \cdots & 0 & 0 \\ \vdots & \vdots & \vdots & \ddots & \vdots & \vdots \\ 0 & 0 & 0 & \cdots & W_{m-1}^{\kappa} & 0 \\ 0 & 0 & 0 & \cdots & 0 & W_m^{\kappa} \end{bmatrix},$$

$$F^{\kappa} = \begin{bmatrix} F_1^{\kappa} \\ F_2^{\kappa} \\ \vdots \\ F_m^{\kappa} \end{bmatrix}, \qquad (Q^*)^{\kappa} = \begin{bmatrix} (Q^*_1)^{\kappa} \\ (Q^*_2)^{\kappa} \\ \vdots \\ (Q^*_m)^{\kappa} \end{bmatrix}.$$

 $W^{\kappa}$  is a composite matrix, where each element is itself a matrix, and the zeros present are zero matrices. The boundary conditions are integrated into the global matrix  $W^{\kappa}$  as follows:

$$\epsilon_1 F_1^{\kappa} = O_{in}, \tag{3.25}$$

$$\epsilon_m F_m^{\ \kappa} = O_{out}, \tag{3.26}$$

where

$$\epsilon_1 = a_{in} \left( \frac{4}{\rho_1 - \rho_0} \right) \psi^*_{1}(\rho_0) D + b_{in} \psi^*_{1}(\rho_0),$$

$$\epsilon_m = a_{out} \left( \frac{4}{\rho_m - \rho_{m-1}} \right) \psi_m^*(\rho_m) D + b_{in} \psi_m^*(\rho_m).$$

Also, interface conditions are integrated in the global matrix, and the matrix form of interface conditions is as follows:

$$T_i F_i^{\kappa} - T_{i+1} F_{i+1}^{\kappa} = 0,$$
 (3.27)

$$R_i F_i^{\kappa} - R_{i+1} F_{i+1}^{\kappa} = 0,$$
 (3.28)

where

$$T_j = \psi_j^* (\rho_j), \quad T_{j+1} = \psi_{j+1}^* (\rho_j), \quad (3.29)$$

$$R_{j} = \sigma_{j} \left( \frac{4}{\rho_{j} - \rho_{j-1}} \right) \psi_{j}^{*} \left( \rho_{j} \right) D, \tag{3.30}$$

$$R_{j+1} = \sigma_{j+1} \left( \frac{4}{\rho_{j+1} - \rho_j} \right) \psi_{j+1}^* \left( \rho_j \right) D. \tag{3.31}$$

To ascertain the composite cylinder's total Page 13 reactivity, the entire system is finally resolved.

# IV. Investigation of stability and error limits

Next, we focus on the analysis of stability and error bounds, commencing with the introduction of the relevant functional spaces.

$$L_2(\Omega_j) = \left\{ H_j : \int_{\Omega_j} H_j^2 d\Omega_j < \infty \right\},\,$$

$$H^1\big(\Omega_j\big)=\big\{H_j\colon H_j, H_j'\in\ L_2\big(\Omega_j\big)\big\}.$$

The subsequent representations illustrate the inner products for  $L_2(\Omega_i)$  and  $H_1(\Omega_i)$  in the given order

$$(H_j, H_i)_{L_2(\Omega_j)} = \int_{\Omega_j} H_j H_i d\Omega_j,$$

$$(H_j, H_i)_{H^1(\Omega_j)} = \int_{\Omega_i} (H_j H_i + H_j' H_i') d\Omega_j,$$

that outlines the definitions of norms.

$$\left\|H_{j}\right\|_{L_{2}\left(\Omega_{j}\right)}^{2}=\left(H_{j},H_{j}\right)_{L_{2}\left(\Omega_{j}\right)},$$

$$\left\|H_j\right\|_{H^1(\Omega_j)}^2 = \left(H_j, H_j\right)_{H^1(\Omega_j)}.$$

#### **Error limitation analysis**

An estimation of the error in layer j is derived, and this approach is consistent across the other layers. The subsequent formula, found in [47], is satisfied by the finite difference method discretization of the fractional partial time derivative in (1.1).

$$D_t^{\lambda} H_i(\rho, t_{\kappa}) = D_{\kappa}^{\lambda} H_i(\rho, t_{\kappa}) + O((\delta t)^{2-\lambda}), \tag{4.32}$$

Therefore, the precise solution of equation (1.1) can be clarified through the following:

$$H_{j}(\rho, t_{\kappa}) = H_{j}^{\kappa}(\rho, t_{\kappa}) + ((\delta t)^{2-\lambda})$$

$$= \varphi_{N}^{x_{j}} H_{j}(\rho, t_{\kappa}) + \varsigma_{N}^{x_{j}} (\rho, t_{\kappa}) + O((\delta t)^{2-\lambda}),$$
(4.33)

In terms of the exact solution for (3.19), it is denoted by  $H_j^K(\rho, t_\kappa)$ . The order N Lagrange polynomial that serves as an interpolant for  $H_j(\rho, t_\kappa)$  across the Chebyshev collocation points  $X_j$  is represented as  $\varphi_N^{X_j} H_j(\rho, t_\kappa)$ . Additionally, the interpolation error, symbolized by  $\varsigma_N^{X_j}(\rho, t_\kappa)$ , is discussed in detail in [39], as shown below.

$$\varsigma_{N}^{X_{j}}(\rho, t_{\kappa}) = \varphi_{N}^{X_{j}} H_{j}(\rho, t_{\kappa}) - H_{j}^{K}(\rho, t_{\kappa}) 
= \frac{H_{j}^{(N+1)}(\xi, t_{\kappa})}{(N+1)!} \vartheta_{N+1}^{X_{j}}(\rho),$$
(4.34)



here,  $\xi$  lies within the interval  $[\rho_{j-1}, \rho_j]$ , and the polynomials  $\vartheta_{N+1}^{X_j}(\rho)$  possess the following composition:

$$\vartheta_{N+1}^{X_j}(\rho) = \prod_{s=0}^N (\rho - \rho_s).$$

It is possible to consider  $\varphi_N^{X_j} H_j(\rho, t_\kappa)$  as a solution to the following problem by using the Lagrange formalism on  $H_j(\rho, t_\kappa)$  in equation (4.33).

$$\delta \left[ \left\langle \mathcal{K}_{N}^{X_{j}} \left( \mathcal{D}(2_{\kappa}) \middle| \lambda \right) \right] \left( \varphi_{N}^{X_{j}} \mathcal{H}_{j} \right) \right]_{N}^{n} \mathcal{D} \left[ t_{\kappa}^{\lambda} \right] \left[ \mathcal{A} F_{j}^{\kappa} \right] + O((\delta t))^{2-\lambda} \right]$$

$$\frac{1}{\rho} \delta t^{\lambda} \mu_{j} \Gamma(2-\lambda) \left( \varphi_{N}^{X_{j}} \mathcal{H}_{j} \right)' (\rho, t_{\kappa}) - \varphi_{N}^{X_{j}} \mathcal{H}_{j} (\rho, t_{\kappa})$$

$$= F_{j}^{\kappa}(\rho) + \Delta F_{j}^{\kappa}(\rho) + O((\delta t)^{2-\lambda}), \tag{4.35}$$

where

$$\Delta F_{j}^{\kappa}(\rho) = \varsigma_{N}^{X_{j}}(\rho, t_{\kappa}) - \delta t^{\lambda} \mu_{j} \Gamma(2 - \lambda) \left(\varsigma_{N}^{X_{j}}\right)^{\prime\prime}(\rho, t_{\kappa}) - \frac{1}{\rho} \delta t^{\lambda} \mu_{j} \Gamma(2 - \lambda) \left(\varsigma_{N}^{X_{j}}\right)^{\prime}(\rho, t_{\kappa})$$

The quantity  $\varphi_N^{X_j} H_j(\rho, t_{\kappa})$  is expressible in Chebyshev series form as  $\varphi_N^{X_j} H_j(\rho, t_{\kappa}) = \psi_j^* \left(Q_j^{*'}\right)^{\kappa}$ , which subsequently gives rise to the discrete Chebyshev series specified to equation (4.35).

$$W_j^{\kappa} \left( Q_j^{*\prime} \right)^{\kappa} = F_j^{\kappa} + \Delta F_j^{\kappa} + O((\delta t)^{2-\lambda}).$$
 (4.36)  
Deducting (3.22) from (4.35) yields

$$|(Q_s^{*\prime})^{\kappa} - (Q_s^{*})^{\kappa}| \lesssim ||W_j^{\kappa}||^{-1} ||\Delta F_j^{\kappa}|| + O((\Delta t)^{2-\lambda}).$$
(4.37)

**Theorem 4.1.** Let's consider  $H_j(\rho, t_{\kappa})$  as the precise solution to (1.1) and  $(H_j)_N(\rho, t_{\kappa})$  as the result obtained from the Chebyshev series applied to (3.19). In light of the effective smoothness of  $H_j(\rho, t_{\kappa})$ , we proceed.

$$\begin{aligned} \left| H_{j}(\rho, t_{\kappa}) - \left( H_{j} \right)_{N}(\rho, t_{\kappa}) \right| \\ &\lesssim \left| \varsigma_{N}^{X_{j}}(\rho, t_{\kappa}) \right| + \left\| \psi_{j}^{*} \right\| \left| W_{j}^{\kappa} \right|^{-1} \left\| \Delta F_{j}^{\kappa} \right\| \\ &+ O((\delta t)^{2-\lambda}). \end{aligned}$$

$$(4.38)$$

**Proof.** Using (4.36), we have determined the error's upper bound as follows:

$$\begin{aligned} \left| H_{j}(\rho, t_{\kappa}) - \left( H_{j} \right)_{N}(\rho, t_{\kappa}) \right| \\ & \leq \left| H_{j}(\rho, t_{\kappa}) - \varphi_{N}^{X_{j}}(\rho, t_{\kappa}) \right| \\ & + \left| \left( \varphi_{N}^{X_{j}}(\rho, t_{\kappa}) - \left( H_{j} \right)_{N}(\rho, t_{\kappa}) \right|, \end{aligned}$$

from (4.34), and the Chebyshev series expansion of  $\varphi_N^{X_j}(\rho, t_\kappa)$  and  $(H_j)_N(\rho, t_\kappa)$  we get

$$\frac{\left|H_{j}(\rho, t_{\kappa}) - \left(H_{j}\right)_{N}(\rho, t_{\kappa})\right| \leq \left|\varsigma_{N}^{X_{j}}(\rho, t_{\kappa})\right| + \left|\psi_{j}^{*}(\rho)\left(Q_{j}^{\mathsf{Page}}\right)^{\kappa} \stackrel{14}{-} \psi_{j}^{*}(\rho)\left(Q_{j}^{*}\right)^{\kappa}\right| + O((\delta t))^{2-\lambda},}$$

$$\leq \left| \varsigma_N^{X_j}(\rho, t_\kappa) \right| + O((\delta t))^{2-\lambda} + \left\| \psi_j^* \right\| \left| \left( Q_j^{*'} \right)^{\kappa} - \left( Q_j^* \right)^{\kappa} \right|,$$

from (4.37) we get

$$\left| H_j(\rho, t_{\kappa}) - \left( H_j \right)_N(\rho, t_{\kappa}) \right| \leq$$

## **Stability**

**Theorem 4.2.** According to equation (3.19), the discretized time numerical scheme is stable without any conditions

**Proof.** The following relation is obtained by assuming  $\omega_j(\rho, t_{\kappa}) = 0$  and multiplying equation (3.19) by  $H_j^{\kappa}$  and integrating it over the domain.

$$(H_{j}^{\kappa}, H_{j}^{\kappa}) - \delta t^{\lambda} \mu_{j} \Gamma(2 - \lambda) \Big( (H_{j}^{\prime\prime})^{\kappa}, H_{j}^{\kappa} \Big)$$

$$- \frac{1}{\rho} \delta t^{\lambda} \mu_{j} \Gamma(2 - \lambda) \Big( (H_{j}^{\prime\prime})^{\kappa}, H_{j}^{\kappa} \Big)$$

$$= (H_{j}^{\kappa-1}, H_{j}^{\kappa})$$

$$- \sum_{L=0}^{\kappa-1} \beta_{L} \Big( (H_{j}^{\kappa-L}, H_{j}^{\kappa}) \Big)$$

$$- (H_{j}^{\kappa-L-1}, H_{j}^{\kappa}) \Big).$$

$$(4.39)$$

Through the application of the Cauchy-Schwarz inequality, we conclude that

$$\left(H_{j}^{\kappa-1}, H_{j}^{\kappa}\right) \leq \frac{1}{2} \left[ \left\| H_{j}^{\kappa-1} \right\|_{L_{2}}^{2} + \left\| H_{j}^{\kappa} \right\|_{L_{2}}^{2} \right] \tag{4.40}$$

Equation (4.39), in conjunction with the Cauchy-Schwarz inequality, produces.

$$\left(1 - \frac{1}{\rho} \delta t^{\lambda} \mu_{j} \Gamma(2 - \lambda)\right) \|H_{j}^{\kappa}\|_{L_{2}}^{2} 
+ \delta t^{\lambda} \mu_{j} \Gamma(2 - \lambda) \left(1 - \frac{1}{\rho}\right) \|\left(H_{j}^{\prime}\right)^{\kappa}\|_{L_{2}}^{2} 
\leq \frac{1}{2} \left[\|H_{j}^{\kappa - 1}\|_{L_{2}}^{2} + \|H_{j}^{\kappa}\|_{L_{2}}^{2}\right] 
+ \frac{1}{2} \sum_{L=0}^{\kappa - 1} \beta_{L} \left[\|H_{j}^{\kappa - L} - H_{j}^{\kappa - L}\|_{L_{2}}^{2} 
+ \|H_{j}^{\kappa}\|_{L_{2}}^{2}\right]$$
(4.41).

Through induction, we establish the stability of equation (3.19). When  $\kappa = 1$ , we find

$$\left(\frac{1}{2} - \frac{1}{\rho} \delta t^{\lambda} \mu_{j} \Gamma(2 - \lambda)\right) \left\|H_{j}^{1}\right\|_{L_{2}}^{2} \leq \frac{1}{2} \left\|H_{j}^{0}\right\|_{L_{2}}^{2}, \quad (4.42)$$



DJERFT., Vol. (1) (II): (P 9 - P18 ) (2025) DOI: 10.21608/djerft.2025.416180.1010

this results in

$$\|H_j^1\|_{L_2}^2 \lesssim \|H_j^0\|_{L_2}^2.$$
 (4.43)

There is a positive real number  $\epsilon$  such that  $D < \epsilon C$   $(D > \epsilon C)$ , as indicated by the expression  $D \lesssim C$   $(D \gtrsim C)$ . A step of induction is in place.

$$\left\| H_{j}^{\kappa-1} \right\|_{L_{2}}^{2} \lesssim \left\| H_{j}^{\kappa-2} \right\|_{L_{2}}^{2} \lesssim \dots \lesssim \left\| H_{j}^{0} \right\|_{L_{2}}^{2}. \tag{4.44}$$

We obtain from (4.41) and (4.44).

$$\left(\frac{1}{2} - \frac{1}{\rho} \delta t^{\lambda} \mu_{j} \Gamma(2 - \lambda)\right) \|H_{j}^{\kappa}\|_{L_{2}}^{2} 
\leq \frac{1}{2} \|H_{j}^{0}\|_{L_{2}}^{2} 
+ \frac{1}{2} \sum_{L=0}^{\kappa-1} \beta_{L} \left[ \|H_{j}^{0}\|_{L_{2}}^{2} + \|H_{j}^{\kappa}\|_{L_{2}}^{2} \right],$$
(4.45)

as seen in [48]  $\sum_{L=0}^{\kappa-1} \beta_L < 1$ , which leads to

$$\|H_j^{\kappa}\|_{L_2}^2 \lesssim \|H_j^0\|_{L_2}^2.$$
 (4.46)

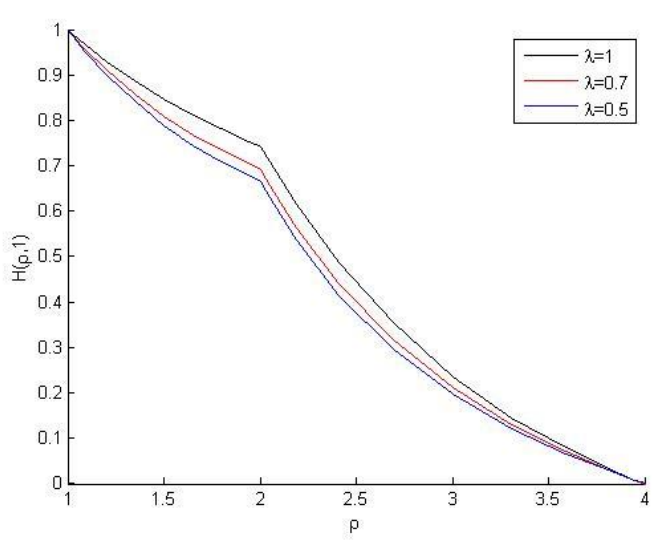
#### V. Numerical experiments

**Example 1:** Examine a two-layer cylinder defined by these parameters:

$$\rho_0 = 1, \quad \rho_1 = 2, \quad \rho_2 = 4,$$
 $\mu_1 = 4, \quad \mu_2 = 1,$ 
 $\sigma_1 = 4, \quad \sigma_2 = 1.$ 

The cylinder maintains fixed temperatures at the inner and outer surfaces:  $H_0 = 4$ ,  $H_2 = 0$ . The initial temperature distribution is zero, and there is no heat generation throughout the cylinder. This design is referenced in [12]. The temperature distributions of the cylinder at t = 1 for fractional order derivatives  $\lambda = 0.5$ , 0.7 are elegantly illustrated in Figure 2. The results at  $\lambda = 1$  align well with those reported in Reference [12].

Figure 2. Distribution of the two-layer cylinder's temperature in example 1 for different values of the fractional-order derivative ( $\lambda$ ) at t = 1.



**Example 2:** Investigate a four-layer cylinder represented by the following parameters

$$\begin{split} \rho_0 &= 0.15, \quad \rho_1 = 0.154, \quad \rho_2 = 0.164, \\ \rho_3 &= 0.214, \quad \rho_4 = 0.216 \\ \mu_1 &= 1.5821e - 5, \quad \mu_2 = 1.6071e - 7, \\ \mu_3 &= 2.9787e - 7, \quad \mu_4 = 8.7232e - 5 \\ \sigma_1 &= 58, \quad \sigma_2 = 0.27, \quad \sigma_3 = 0.056, \quad \sigma_4 = 209 \\ a_{in} &= -58, \quad a_{out} = 209, \quad b_{in} = 4, b_{out} = 25 \\ o_{in} &= 72, \\ o_{out} &= 16500(1 - 0.678e^{-0.32t} - 0.313e^{-3.8t}) + 450 \end{split}$$

The structure's temperature at the initial time is  $18^{\circ}$ C. Table 1 shows the temperature distribution of example 2 at different distance coordinates ( $\rho$ ) for both the Chebyshev collocation method and the Fourier method [49]. The obtained results demonstrate that the two approaches yield close temperature values within the distance range, although some differences exist. The two approaches reveal good consistency in predicting temperature distribution.

Table 1. Temperature Distribution Results from Chebyshev Collocation and Fourier Methods for example 2 at t = 600 sec,  $\lambda = 1$ 

ρ	Chebyshev collocation method	Fourier method [49]
0.15	19.15	19.1
0.154	20.8	21
0.164	47.65	47.7



DJERFT., Vol. (1) (II): (P 9 - P18 ) (2025) DOI: 10.21608/djerft.2025.416180.1010

0.17	101.97	102
0.2	195.05	195
0.214	340.02	340
0.216	618	618

Figure 3 shows the temperature profile over the radial direction of a composite cylinder in example 2 for various numerical values of  $\lambda$ . The classical curve ( $\lambda=1$ ) exhibits a linear temperature decrease, representing the predicted temperature profile from the conventional Fourier's law. On the other hand, the small values for the fractional indexes,  $\lambda=0.5$  and  $\lambda=0.2$ , yield a stronger nonlinearity for the temperature profile, indicating how fractional calculus models could smoothly include anomalous diffusion and memory in concrete systems. This deviation from the classic behavior describes the model's ability to explain more complex heat conduction phenomena.

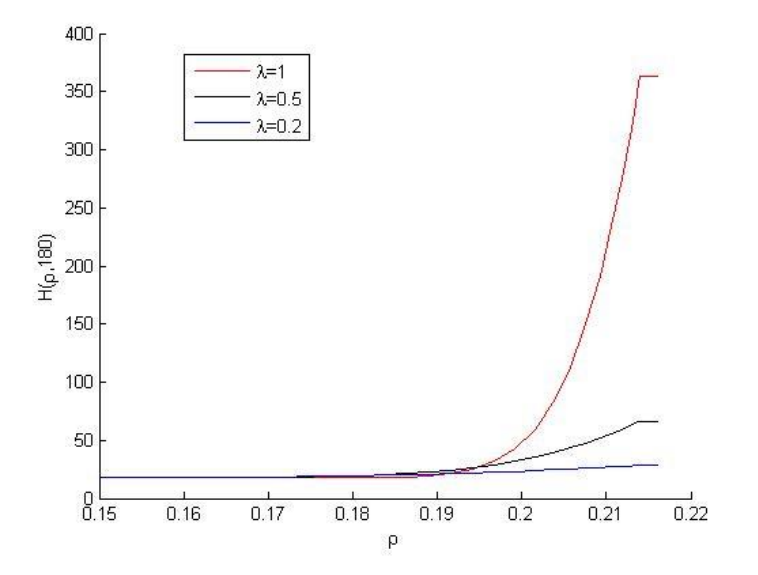


Figure 3. Temperature distribution across the four lavers of a composite cylinder in example 2 for different values of the fractional-order derivative ( $\lambda$ ) at t = 180 sec

**Example 3:** Let's analyze a two-layer cylinder defined by these parameters:

$$\rho_0 = 0.5, \quad \rho_1 = 1, \quad \rho_2 = 2,$$

$$\mu_1 = 1, \quad \mu_2 = 2,$$

$$\sigma_1 = 2, \quad \sigma_2 = 1.$$

 $\omega_1(\rho,t)$  and  $\omega_2(\rho,t)$  are chosen so the exact solution of (1.1) is given by

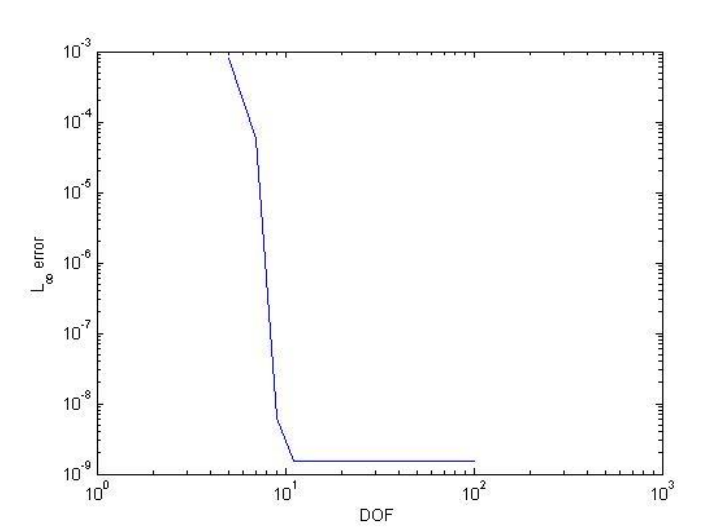
$$H(\rho,t) = \begin{cases} \frac{1}{600}(t+t^2)\rho^4 & \text{Page 16} \\ \frac{1}{600}(t+t^2)(2\rho^4 - 1) & \rho \in (1,2) \end{cases}$$

We have selected parameters that may not correspond to a physical situation; however, since the primary objective in this example is to verify the accuracy of our numerical approach, we will use the analytical results and the traces to compare both exact and numerical solutions. Table 2 illustrates the spectral accuracy of the Chebyshev collocation method for example 3 at  $\lambda = 0.5$ . The main finding, we have is that a remarkably low error of order  $10^{-9}$  can be achieved with very few collocation points. This swift convergence demonstrates the high efficiency of the method without the necessity of large computational grids. Then the error saturates for  $N \ge 11$ . It is this property that makes the Chebyshev method so effective in obtaining very accurate solutions with a small number of computations.

Table 2.  $L_{\infty}$  error of solution for example 2 at  $\lambda = 0.5$ ,  $\delta t = 0.001$ 

N	Chebyshev collocation method $L_{\infty}$ error
5	8.05e-04
7	5.81e-05
9	6.23e-09
11	1.52e-09
21	1.52e-09
31	1.52e-09

Figure 4 plots the convergence behavior of the Chebyshev collocation approach for example 3 at  $\lambda = 0.5$ , showing how the error in the result decreases as computational effort





(measured in Degrees of Freedom (DOF)) increases

Figure 4.  $L_{\infty}$  error of solution for example 2 versus DOF at  $\lambda = 0.5$ ,  $\delta t = 0.001$ 

#### VI. CONCLUSION

The present study reports an application of the Chebyshev collocation technique for solving the fractional temporal heat transfer model in hollow composite cylinders. We discretize terms associated with derivatives with respect to time and space using the first-order finite difference scheme and Chebyshev collocation method, respectively. An a priori error estimate of the proposed method was obtained. In addition, we conducted numerical tests for a two-layer cylinder, and our simulation results were more in agreement with those obtained and described in other literature. There are limitations for the Chebyshev collocation method. In particular, its computational efficiency can be impacted by the dense matrices generated for complex problems, and its accuracy is extremely sensitive to solution smoothness, which may not be met at material interfaces in the composite. In future work, we plan to address these issues by considering domain decomposition to treat material interfaces and by investigating efficient iterative solvers for the generated dense problems.

#### VII. Declarations

#### **Funding**

The author did not receive any funds to help with the preparation of this manuscript.

## **Data availability**

No datasets were generated or analyzed during the current study

## **Conflicts of interest**

The authors declare that they have no competing interests.

## **REFERENCES**

- S. Singh and P. K. Jain, Analytical solution of time-dependent multilayer heat conduction problems for nuclear applications, 2010 1st International Nuclear & Renewable Energy Conference (INREC), IEEE, 2010, pp. 1-6.
- F. J. Pena and M. J. de Lemos, Numerical investigation of an innovative through-tubing solution to thermal plug and abandonment of oil wells with thermite reactions, Applied Thermal Engineering 254 (2024), 123874.
- G. Zhang, C. Xia, M. Sun, Y. Zou, S. Xiao, A new model and analytical solution for the heat conduction of tunnel lining ground heat exchangers, Cold Reg. Sci. Technol. 88 (2013) 59–66..

- L. B. Kong, Z. Li, L. Liu, R. Huang, M. Abshinova, Z. Yangage Tang, P. Tan, C. Deng and S. Matitsine, Recent progress in some composite materials and structures for specific electromagnetic applications, International Materials Reviews 58 (2013), no. 4, 203-259.
- L. Dobrzański, M. Drak and B. Ziębowicz, New possibilities of composite materials application—materials of specific magnetic properties, Journal of Materials Processing Technology 191 (2007), no. 1-3, 352-355.
- J.C. Jaeger, Some problems involving line sources in conduction of heat, London Edinburgh Dub. Phil. Mag. J. Sci. 242 (1944) 169–179
- M. Li, A.C.K. Lai, Analytical model for short-time responses of borehole ground heat exchangers: model development and validation, Appl. Energy 104 (2013) 510–516.
- X. Lu, P. Tervola, M. Viljanen, A new analytical method to solve heat equation for multi-dimensional composite slab, J. Phys. A: Math. Gen. 38 (2005) 2873–2890.
- X. Lu, P. Tervola, M. Viljanen, Transient analytical solution to heat conduction in multi-dimensional composite cylinder slab, Int. J. Heat Mass Transfer 49 (2006) 1107–1114.
- M.D. Mikhailov, M.N. Ozisik, Transient conduction in a threedimensional composite slab, Int. J. Heat Mass Transfer 29 (1986) 340– 342.
- 11. C.W. Tittle, Boundary value problems in composite media: quasiorthogonal functions, J. Appl. Phys. 36 (4) (1965) 1486–1488.
- M.D. Mikhailov, M.N. Ozisik, N.L. Vulchanov, diffusion in composite layers with automatic solution of the eigenvalue problem, Int. J. Heat Mass Transfer 26 (1983) 1131–1141.11.
- P.E. Bulavin, V.M. Kashcheev, Solution of nonhomogenous heatconduction equation for multilayer bodies, Int. Chem. Eng. 5 (1) (1965) 112–115.
- Y. Yener, M.N. Ozisik, On the solution of unsteady heat conduction in multiregion finite media with time-dependent heat transfer coffecient, Proceeding of the Fifth International Heat Transfer Conference, vol. 1, JSME, Tokyo, 1974, pp. 188–192.
- Kevin D. Cole, A. Haji-Sheikh, James V. Beck, Bahman Litkouhi, Heat Conduction Using Green's Function, Taylor and Francis Group, LLC. 2011.
- Haji-Sheikh, J.V. Beck, Temperature solution in multidimensional multi-layer bodies, Int. J. Heat Mass Transfer 45 (2002) 1865–1877.
- I. Ahmadi, M.M. Aghdam, Heat transfer in composite materials using a new truly local meshless method. International Journal of Numerical Methods for Heat & Fluid Flow. 21 (3) (2011) 293–309.
- Y. Povstenko, J. Klekot, Time-fractional heat conduction in two joint half-planes, Symmetry. 11(6) (2019) 800.
- Y. Povstenko, Time-fractional heat conduction in a two-layer composite slab. Fractional Calculus and Applied Analysis. 19(4) (2016) 940-953.
- J. Ma., Y. Sun, J. Yang, Analytical solution of dual-phase-lag heat conduction in a finite medium subjected to a moving heat source. International Journal of Thermal Sciences. 125 (2018) 34-43.
- G. Xu, J. Wang, Analytical solution of time fractional Cattaneo heat equation for finite slab under pulse heat flux. Applied Mathematics and Mechanics. 39(10) (2018) 1465-1476.
- X.-Y. Zhang, X.-F. Li, Transient response of a functionally graded thermoelastic plate with a crack via fractional heat conduction. Theoretical and Applied Fracture Mechanics, 104 (2019) 102318.
- S. Kukla, U. Siedlecka, An analytical solution to the problem of timefractional heat conduction in a composite sphere. Bulletin of the Polish Academy of Sciences: Technical Sciences. 65(2) (2017) 179-186.
- S. Kukla, U. Siedlecka, Fractional heat conduction in a sphere under mathematical and physical Robin conditions. Journal of Theoretical and Applied Mechanics. 56(2) (2018) 339-349.
- B. Datsko, I. Podlubny, Y. Povstenko, Time-fractional diffusion-wave equation with mass absorption in a sphere under harmonic impact. Mathematics. 7(5) (2019) 433.
- T.-H. Ning, X.-Y. Jiang, Analytical solution for the time-fractional heat conduction equation in spherical coordinate system by the method of variable separation. Acta Mechanica Sinica. 27 (2011) 994-1000.
- B. Yu, X. Jiang, Temperature prediction by a fractional heat conduction model for the bi-layered spherical tissue in the



- hyperthermia experiment. International Journal of Thermal Sciences. 145 (2019) 105990.
- X. Jiang, M. Xu, The time fractional heat conduction equation in the general orthogonal curvilinear coordinate and the cylindrical coordinate systems, Physica A. 389 (2010) 3368-3374.
- Y. Povstenko, Time-fractional radial heat conduction in a cylinder and associated thermal stresses. Archive of Applied Mechanics. 82 (2012) 345-362.
- Y. Povstenko, Axisymmetric solution to time-fractional heat conduction equation in an infinite cylinder under local heating and associated thermal stresses, International Journal of Mechanics. 8(1) (2014) 383-390.
- M. A. Ezzat, A. A. El-Bary, Effects of variable thermal conductivity and fractional order of heat transfer on a perfect conducting infinitely long hollow cylinder. International Journal of Thermal Sciences. 108 (2016) 62-69.
- S. Blasiak, Time-fractional Fourier law in a finite hollow cylinder under Gaussian-distributed heat flux, EPJ Web of Conferences. 180 (2018) 02008.
- E. Adel, I. L. El-Kalla, A. Elsaid, M. Sameeh, An Adaptive Finite Element Scheme for Solving Space-time Riesz-Caputo Fractional Partial Differential Equations, Iran. J. Sci. 49 (2025) 1061–1073.
- M. El-Borhamy, Numerical study of the stationary generalized viscoplastic fluid flows, Alexandria Engineering Journal.57(3) (2018) 2007-2018.
- M. Sezer, M. Kaynak., Chebyshev polynomial solutions of linear differential equations. Internat J Math Ed Sci Tech.27 (1996) 607–611.
- A. Akyüz, M. Sezer. Chebyshev polynomial solutions of systems of high-order linear differential equations with variable coefficients. J Comput Appl Math. 144 (2003) 237–247.
- A. Akyüz-Yaslan, H. Çerdk-yaslan. The solution of high-order nonlinear ordinary differential equations by Chebyshev series. Jc omput Appl Math.127 (2011) 5658–5666.
- C. Keşan, Chebyshev polynomial solutions of second-order linear partial differential equations. Appl Math Comput. 134 (2003) 109– 124.
- G. Yuksel, O. Rasil, M. Sezar. Error analysis of the Chebyshev collocation method for linear second-order partial differential equations. Int J Comput Math. 92 (2015) 2121–2138.
- MP. Mkhatshwa, M. Khumalo, PG. Dlamini. Multi-domain multivariate spectral ollocation method for (2+1) dimensional nonlinear partial differential equations. Partial Differential Equations Appl Math. 6 (2022) 100440.
- M. El-Gamel, M. Sameeh. A Chebyshev collocation method for solving Troesch's problem. Int J Math Comput Appl Res. 2013;3:23– 32.
- M. Sameeh, A. Elsaid. Chebyshev collocation method for parabolic partial integro differential equation. J Adv Math Phys. 2016:7854806.
- A. Akyüz, M.Sezer. A Chebyshev collocation method for the solution of linear integro differential equations. J Comput Math. 72 (1999) 491–507.
- JK. Mohammed, AR. Khudair. Integro-differential equations: Numerical solution by a new operational matrix based on fourth-order hat functions. Partial Differential Equations Appl Math. 8 (2023) 100529
- H. Çerdk-yaslan, A. Akyüz-Yaslan. Chebyshev polynomial solution of non-linear fredholm-Volterra integro-differential equations. J Arts Sci. 6 (2006) 89–101.
- M. El-Gamel, M. Sameeh. An efficient technique for finding the eigenvalues of fourth-order Sturm-Liouville problems. Appl Math. 3 (2012) 920–925.
- M. Stynes, E. O'riordan, J.L. Gracia, Error analysis of a finite difference method on graded meshes for a time-fractional diffusion equation, SIAM J. Numer. Anal. 55 (2017) 1057–1079.
- B. Sagar, S.S. Ray, Numerical soliton solutions of fractional Newell— Whitehead–Segel equation in binary fluid mixtures, Comput. Appl. Math. 40 (2021) 290.
- R. M. Tatsii, O.Y Pazen, Direct (Classical) Method of Calculation of the Temperature Field in a Hollow Multilayer Cylinder, J Eng Phys Thermophy. 91 (2018) 1373–1384.